

Global Phase Diagram and Momentum Distribution of Single-Particle Excitations in Kondo insulators

J. H. Pixley,¹ Rong Yu,^{2,3} Silke Paschen,⁴ and Qimiao Si⁵

¹*Condensed Matter Theory Center and Joint Quantum Institute, Department of Physics, University of Maryland, College Park, Maryland 20742-4111 USA*

²*Department of Physics, Renmin University of China, Beijing, 100872, China*

³*Department of Physics and Astronomy, Collaborative Innovation Center of Advanced Microstructures, Shanghai Jiaotong University, Shanghai 200240, China*

⁴*Institute of Solid State Physics, Vienna University of Technology, Wiedner Hauptstraße 8-10, 1040 Vienna, Austria*

⁵*Department of Physics & Astronomy, Rice University, Houston, Texas, 77005, USA*

(Dated: October 29, 2018)

Kondo insulators are emerging as a simplified setting to study both magnetic and metal-to-insulator quantum phase transitions. Here, we study a half-filled Kondo lattice model defined on a magnetically frustrated Shastry-Sutherland geometry. We determine a “global” phase diagram that features a variety of zero-temperature phases; these include Kondo-destroyed antiferromagnetic and paramagnetic metallic phases in addition to the Kondo-insulator phase. Our result provides the theoretical basis for understanding how applying pressure to a Kondo insulator can close its hybridization gap, liberate the local-moment spins from the conduction electrons, and lead to a magnetically correlated metal. We also study the momentum distribution of the single-particle excitations in the Kondo insulating state, and illustrate how Fermi-surface-like features emerge as a precursor to the actual Fermi surfaces of the Kondo-destroyed metals. We discuss the implications of our results for Kondo insulators including SmB_6 .

PACS numbers: 71.10.Hf, 71.27.+a, 75.20.Hr

Quantum criticality in the vicinity of antiferromagnetic order is of interest to a variety of strongly correlated electron systems [1]. Heavy fermion systems occupy a special place in this context [2, 3]. These systems are typically described by a Kondo lattice model, which contains a lattice of local-moment spins coupled to a band of conduction electrons. The strong interactions, which underlie the local moments, allow the ground states of these systems to be readily tuned by external parameters such as pressure or magnetic field. For this reason, antiferromagnetic (AF) quantum critical points (QCPs) have been identified in a host of heavy fermion metals. Experimental studies at such QCPs [4–7] have provided evidence for a Kondo-destruction local QCP [8–10], across which the Fermi surface jumps from “large” (incorporating the f -electrons) to “small” (excluding the f -electrons). Experimental efforts have also been devoted to heavy fermion metals that allow a systematic tuning of inherent quantum fluctuations, through strong magnetic frustration [11–15], dimensionality [16] or other related means [17–19], which are shedding light on novel phases that involve the development or destruction of not only the AF order parameters but also the Kondo entanglement. Such effects have been theoretically considered, and a global phase diagram has been advanced [20–23].

In the context of such developments in heavy-fermion metals it is then a natural question to ask, whether and how quantum phase transitions can be realized in Kondo insulators [24]? When the local-moment spins form a Kondo singlet with the spins of the conduction electrons,

the resulting Kondo resonances are described in terms of a hybridization with the conduction electrons [25]. An incommensurate electron-filling implies that the chemical potential intersects the hybridized bands, which leads to a heavy-fermion metallic state. By contrast, for a commensurate filling, the chemical potential falls in the middle of a hybridization gap [26, 27], and a Kondo-insulator state ensues. If, by analogy with the case of the heavy fermion metals, an external parameter such as pressure tunes the system across a Kondo-destruction transition, the gap of the Kondo insulator will close. At the same time, the local-moment spins will be liberated from the conduction electrons, thereby yielding magnetic states in which the spin-rotational invariance is either spontaneously broken (*e.g.*, an AF order) or preserved (a valence-bond solid or a spin liquid). This type of qualitative considerations have led to a proposed global phase diagram for Kondo insulators [28], but systematic theoretical studies have yet to be performed to map this out.

Studies along this direction are also important to understand the on-going experiments on Kondo insulators [24], which in recent years have been particularly fueled by the search for topological Kondo insulating states [29] in SmB_6 and related systems. Two types of experiments have added to the motivation for the present work. First, it is known that applying pressure drives SmB_6 from a Kondo insulator to an AF metal [30], with indications for linear resistivity near the threshold pressure [31]. Second, torque magnetometry measurements have observed a de Haas-van Alphen signal in

SmB₆ [32, 33], raising the exciting possibility that the Kondo insulator state harbors an incipient Fermi surface of the underlying conduction electrons [33].

In this paper, we study a half-filled Kondo lattice model. First, in order to have a convenient tuning parameter for quantum fluctuations of the local-moment magnetism, we focus on the model defined on the geometrically frustrated Shastry-Sutherland lattice. The calculated phase diagram is strikingly similar to the global phase diagram proposed earlier based on qualitative considerations [28]. Second, we study the momentum distribution of single-particle excitations in the Kondo insulating state. We identify a Fermi-surface-like feature in the Kondo insulating phase, and show how it represents a *precursor* to the actual Fermi surfaces of the Kondo-destroyed metals that are “nearby” in the zero-temperature phase diagram.

The half filled (*i.e.* one conduction electron per site) Kondo-Heisenberg model is defined as

$$H = \sum_{(i,j),\sigma} t_{ij}(c_{i\sigma}^\dagger c_{j\sigma} + \text{h.c.}) + J_K \sum_i \mathbf{S}_i \cdot \mathbf{s}_i^c + \sum_{(i,j)} J_{ij} \mathbf{S}_i \cdot \mathbf{S}_j \quad (1)$$

where (i, j) denotes a sum over neighboring bonds, with a hopping strength t_{ij} , an RKKY interaction J_{ij} , and a Kondo coupling J_K . The spin density of the conduction electrons at site i is $\mathbf{s}_i^c = c_{i\alpha}^\dagger (\boldsymbol{\sigma}_{\alpha\beta}/2) c_{i\beta}$, where $\boldsymbol{\sigma}_{\alpha\beta}$ are the Pauli spin matrices, which are Kondo coupled (via $J_K > 0$) to spin-1/2 local moments, $\mathbf{S}_i = f_{i\alpha}^\dagger (\boldsymbol{\sigma}_{\alpha\beta}/2) f_{i\beta}$. To represent the spins, we use fermionic spinons [34] $f_{i\sigma}$ which are subject to the constraint $\sum_\sigma f_{i\sigma}^\dagger f_{i\sigma} = 1$. The half filled condition is $n_c = 1$, where $n_c = \frac{1}{N} \sum_{i,\sigma} \langle c_{i\sigma}^\dagger c_{i\sigma} \rangle$ is the filling of the conduction band (N is the number of sites in the lattice).

Global phase diagram: We consider the two-dimensional (2D) Kondo lattice model on the SSL geometry, which is depicted in Fig. 1. Here J_1 and J_2 denote the nearest neighbor (NN) and next nearest neighbor (NNN) RKKY interactions, respectively, and t_1 and t_2 are for the NN and NNN hoppings, respectively. In the limit of $J_K = 0$ both the Heisenberg model on the SSL [35, 36] and the electronic band structure have been studied [37, 38] in detail. It is known that for $J_2/J_1 > 2$ the SSL Heisenberg model exhibits an exact valence bond solid (VBS) ground state. In the incommensurate-filling case, quantum phase transitions between the heavy-fermion metal phase and other magnetic-metal phases have been studied [23, 39, 40].

We treat the Kondo interaction by introducing a Hubbard-Stratonovich decoupling in the Kondo-singlet (*i.e.* hybridization) channel $B_i = \sum_\sigma c_{i\sigma}^\dagger f_{i\sigma}$. In addition, to capture the valence bond solid (VBS) and AF orders, we split the Heisenberg interaction into each of these respective channels written as $D_{ij} = \sum_\sigma f_{i\sigma}^\dagger f_{j\sigma}$ and $\mathbf{S}_i = f_{i\alpha}^\dagger (\boldsymbol{\sigma}_{\alpha\beta}/2) f_{i\beta}$, and we weight the channels by a parameter x , where $0 < x < 1$ [23]. This leads to the

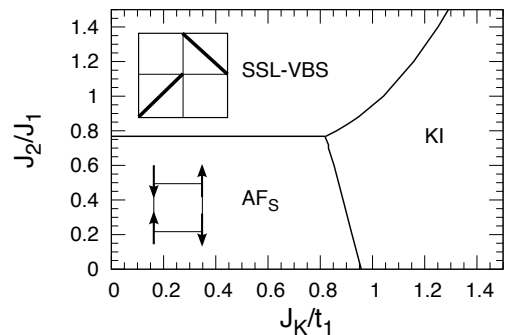


FIG. 1. Zero temperature phase diagram as a function of frustration (J_2/J_1) and Kondo coupling (J_K/t_1), for half filling $n_c = 1.0$ and for $t_2/t_1 = 0.25$. The phases and their transitions are described in the main text.

mean field Hamiltonian

$$H_{MF} = C - \sum_i (b_i^* c_{i\sigma}^\dagger f_{i\sigma} + \text{h.c.}) + \sum_i \lambda_i f_{i\sigma}^\dagger f_{i\sigma} \quad (2)$$

$$+ \sum_{(i,j)} \left([(t_{ij} c_{i\sigma}^\dagger c_{j\sigma} - Q_{ij}^* f_{i\sigma}^\dagger f_{j\sigma}) + \text{h.c.}] + \tilde{J}_{ij} 2\mathbf{M}_i \cdot \mathbf{S}_j \right)$$

where the sum over σ is implied, and we have defined $\tilde{J}_{ij} = (1-x)J_{ij}$. The constant term is $C = \sum_i (2|b_i|^2/J_K - \lambda_i) + \sum_{(i,j)} (2|Q_{ij}|^2/(xJ_{ij}) - \tilde{J}_{ij} \mathbf{M}_i \cdot \mathbf{M}_j)$. The hybridization is $b_i = J_K \langle B_i \rangle / 2$, and the Hubbard-Stratonovich parameters in the resonating valence bond (RVB) singlet channel are $Q_{ij} = x J_{ij} \langle D_{ij} \rangle / 2$. Lastly, the AF order parameter is $\mathbf{M}_i = \langle \mathbf{S}_i \rangle$ [with the ordering wave vector $\mathbf{Q} = (\pi, \pi)$]. We solve for these parameters as described in Ref. [23] using a four site unit cell labelled by $X = A, B, C, D$, with the corresponding four constraints and Kondo hybridization λ_X and b_X respectively. This leads to ten RVB parameters $Q_{x_i}, Q_{y_i}, Q_{x+y}$, and Q_{x-y} where $i = 1-4$ and the geometry is specified in Ref. [23]. We determine the zero temperature phase diagram for various different values of t_2/t_1 , and fix $x = 0.7$. This choice of x is guided by the magnetic phase diagram at $J_K = 0$, where taking $x = 0.7$ captures the quantum AF ground state (in the limit of $J_2 = 0$) [23]; taking this solution as a candidate state we have checked that our results discussed below are robust within a certain range of x .

In Fig. 1, we show the phase diagram for $t_2/t_1 = 0.25$, which reveals the three relevant phases. For small J_K/t_1 and J_2/J_1 the model is in the AF phase, defined by $0 < |\mathbf{M}| < 1/2$. Here, Q_{ij} is only non-zero along the vertical and horizontal bonds and $b_X = 0$. As this phase has no Kondo screening and is antiferromagnetic we dub it AF_S , where the S denotes a small Fermi surface. In the limit of large frustration and small J_K/t_1 the model gives rise to the expected SSL-VBS, where Q_{x+y} and Q_{x-y} are the only non-zero singlet parameters. In the limit of large Kondo coupling we find a Kondo insulating (KI) phase. Here all the Q_{ij} and b_X are non-zero, and they preserve

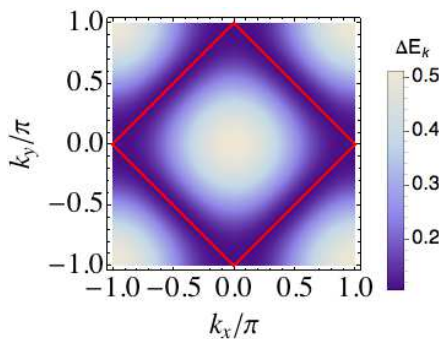


FIG. 2. (Color online). Effects of the underlying Fermi surface on the band gap in the KI phase. The band gap $\Delta E_{\mathbf{k}}$ is plotted in momentum space for $J_K/t = 1.5$ in the KI phase. The minimum of the band gap is along the underlying small Fermi surface (the same as for $J_K = 0.0$), corresponding to the diamond marked in red.

the symmetry of the Shastry-Sutherland lattice.

We find direct transitions between AF_S and KI, as well as between SSL-VBS and KI. In the incommensurate-filling case [23], we found various intermediate phases (between the VBS and heavy Fermi liquid) that break the underlying symmetry of the Shastry-Sutherland lattice and as a result exhibit partial Kondo screening. Here, we find these solutions to be energetically not competitive. While our approach yields first order transitions (see the Supplementary Material [41]), it is important to see how the fluctuation effects beyond our approach affect the nature of the transitions. Based on the studies [42] on the quantum fluctuations in pertinent quantum impurity models in the context of extended dynamical mean field approach [8, 10], we expect the transitions to be continuous.

Two remarks are in order. First, the phase diagram we have found is strikingly similar to the global phase diagram proposed for Kondo insulators on qualitative grounds [28]. From a more general point of view, we can think of J_2/J_1 as a measure of the strength of quantum fluctuations in the system. Therefore, the phase diagram we have derived is representative of Kondo insulating systems more generally; for instance, dimensionality tuning could serve for a similar purpose [16]. Second, each type of phase transition between the KI phase and either the AF_S or the SSL-VBS is actually a *metal to insulator* transition. Thus, there should be significant effects on Fermi surface probes as the transition is approached from the metallic side as well as from the insulating side, on which we now turn to.

Single-particle excitations and precursor of the small Fermi surface in the KI phase: We focus on the KI phase itself to consider the momentum distribution of the single-particle excitations. We are primarily interested in what effects the underlying Fermi surface of the conduction electrons have “imprinted” on the properties

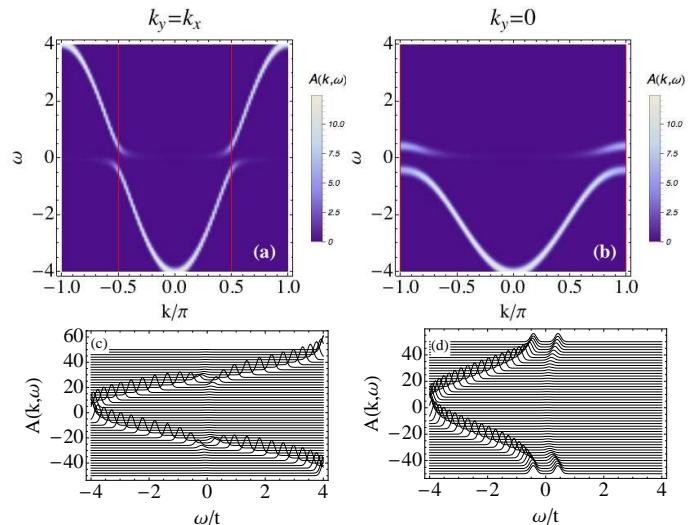


FIG. 3. (Color online). The spectral function for $J_K/t_1 = 1.5$ along the content momentum cuts (a) $k = k_y = k_x$ and (b) $k = k_x, k_y = 0$, the red lines mark the location of the small Fermi momentum k_F . Energy dispersion curves of the spectral function are shown along the momentum cuts (c) $k = k_y = k_x$ and (d) $k = k_x, k_y = 0$. Here, each curve is shifted vertically by an integer corresponding to the wavenumber index and we have broadened the delta function by a Gaussian of width $0.1t$.

of the insulating state. For definiteness, we will denote such small Fermi momenta by \mathbf{k}_F , and the large Fermi momenta (those that incorporate the f -electrons, see below) by \mathbf{k}_F^* . To make concrete connections, we now restrict ourselves to a model defined on a 2D square lattice with NN couplings only, and therefore consider one site per unit cell. In addition, for the KI phase where the magnetic order parameter vanishes, we no longer consider the effects of the Heisenberg term in Eq. (1) and set $J_1 = J_2 = 0$; this still keeps the salient properties of the momentum distribution in this phase. Note that in the following we only have one hopping parameter t and we drop the subscript “1” in the remainder of the paper.

We first consider the hybridization gap $\Delta E_{\mathbf{k}}$ as a function of momentum. Solving for the band structure in the square lattice case yields two bands $E_{\mathbf{k}\pm} = \frac{1}{2}(\epsilon_{\mathbf{k}} - \lambda) \pm \sqrt{\left(\frac{\epsilon_{\mathbf{k}} + \lambda}{2}\right)^2 + b^2}$, where $\epsilon_{\mathbf{k}} = -2t(\cos k_x + \cos k_y) - \mu$ is the dispersion with a bandwidth $W = 8t$ and chemical potential μ . A Kondo insulator of course has no Fermi surface. However, plotting the direct hybridization gap $\Delta E_{\mathbf{k}} \equiv E_{\mathbf{k}+} - E_{\mathbf{k}-}$ as a function of \mathbf{k} in the entire Brillouin zone reveals a special surface (line) in the Brillouin zone. As shown in Fig. 2, $\Delta E_{\mathbf{k}}$ is minimized along the diamond marked in red, which corresponds to the small Fermi surface for the half-filled conduction-electron band, $n_c = 1$. We therefore reach one of our main results, namely $\Delta E_{\mathbf{k}}$ is *minimized on the small Fermi momenta*, \mathbf{k}_F . The magnitude of the direct (and indirect) gap is

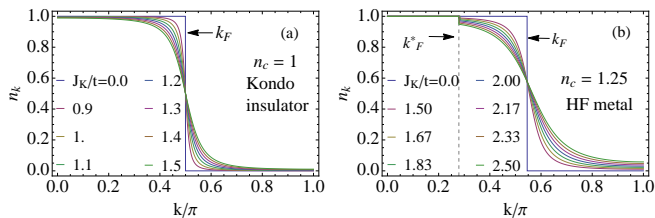


FIG. 4. (Color online). Momentum distribution of the c electrons $n_{\mathbf{k}}$, for $k = k_x = k_y$. $n_{\mathbf{k}}$ versus k for various Kondo couplings in the KI phase (a) and the metallic phase with $n_c = 1.25$ (b). The overall shape across k_F in both cases is discussed in the text, while for the metal there is a jump at the large Fermi wave-vector k_F^* (dashed line) of the size of the quasiparticle residue.

discussed in the Supplementary Material (Ref. [41]).

To further illustrate the role played by the small Fermi momenta \mathbf{k}_F , we consider the dispersion of the single particle excitations and momentum evolution of the conduction-electron spectral function $A(\mathbf{k}, \omega) = -\text{Im}G_c(\mathbf{k}, \omega)/\pi$ (see the Supplemental Material [41]) as shown in Fig. 3. Along the cut $k_x = k_y$, as shown in Fig. 3(a), we find the quasiparticle states dispersing towards the small Fermi momentum $\mathbf{k}_F = (\pi/2, \pi/2)$ as the Fermi energy is approached, although they are eventually gapped out by the hybridization when \mathbf{k} gets too close to \mathbf{k}_F . This point is also illustrated in the energy dispersion curves, shown in Fig. 3(c). The same trend is also observed for the momentum cut $k_y = 0$, Figs. 3 (b) and (d), although here the small Fermi momentum is $\mathbf{k}_F = (\pi, 0)$, which is located on the zone boundary.

To appreciate the above observations, we note that the small Fermi momenta \mathbf{k}_F are special because, for $J_K = 0$, the momentum distribution of the c electrons, $n_{\mathbf{k}} = \sum_{\sigma} \langle c_{\mathbf{k},\sigma}^{\dagger} c_{\mathbf{k},\sigma} \rangle$, has a jump of exactly 1 across such momenta. A non-zero Kondo coupling will smear this jump [25], but this smearing occurs gradually. Indeed, as shown in Fig. 4 (a), near the small Fermi momentum \mathbf{k}_F , for various values of the Kondo coupling in the KI phase, we see a step function for $J_K = 0$ develop into an ‘‘S-shape’’ pinned at \mathbf{k}_F with increasing J_K . (Without a loss of generality, we consider the trajectory in the Brillouin zone $0 < k_x = k_y < \pi$.) This smeared jump in the momentum distribution of the occupation number at \mathbf{k}_F is caused by the same physics that induces the small excitation gap at \mathbf{k}_F illustrated in Figs. 2 and 3.

The simplicity of the Kondo insulator is that the large Fermi momenta, \mathbf{k}_F^* , are located at the Brillouin zone boundary. This is to be contrasted with the incommensurate-filling case, as illustrated in Fig. 4(b) for $n_c = 1.25$. In this case, the features at the small Fermi momenta, \mathbf{k}_F , remain similar to the Kondo-insulator case. However, now, \mathbf{k}_F^* occurs in the middle of the Brillouin zone. As is characteristic of a heavy-fermion metal [25], $n_{\mathbf{k}}$ display a sharp drop at \mathbf{k}_F^* . The drop

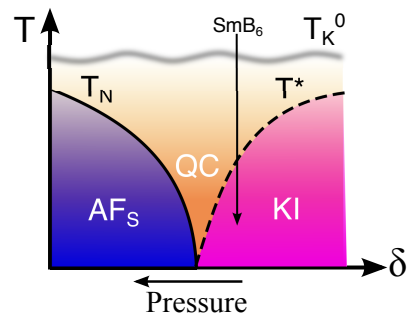


FIG. 5. (Color online). Schematic finite temperature phase diagram as a function of the control parameter δ . The close proximity of the Kondo-insulator (KI) state to a Kondo-destroyed AF phase (AF_S) gives rise to a zero temperature quantum critical (QC) and a concomitant quantum critical (QC) regime.

is tiny, measuring the exponentially small quasiparticle residue.

Discussion and outlook: We now explore the implications of the global phase diagram shown in Fig. 1. By tuning various Kondo insulating compounds (e.g. under pressure) into and out of various ground states, this phase diagram opens up the exciting possibility of realizing new types of quantum phase transitions. From the Kondo-insulating state, such tuning can suppress the insulating gap by destroying the Kondo effect, liberate the local-moment spins, and give rise to either an AF or paramagnetic metallic phase. In these metallic phases, the Fermi surface is small as defined earlier, namely it incorporates only the conduction electrons but not the f -electrons.

Taking a cut in the global phase diagram provides the basis to construct a schematic finite temperature phase diagram. We illustrate this point in Fig. 5 on the case when, along the chosen cut, the Kondo-destroyed phase nearby to the Kondo insulator is AF_S . The AF order is destroyed at the Néel temperature T_N , whereas the Kondo insulating state persists up to a renormalized effective Kondo energy scale T^* , which is distinct from the much higher in energy bare single ion Kondo temperature T_K^0 , due to a renormalization from the presence of the RKKY interaction. Thus at finite temperature, by tuning an external control parameter (δ) the system can go from an AF_S phase into a cross over regime driven by the zero temperature quantum critical (QC) fluctuations, which then crosses over to the KI phase at T^* . Starting from high temperature for a control parameter that is in the KI phase at zero temperature, lowering the temperature through T_K^0 leads into the QC regime and non-trivial scaling features, which then become cut off by the Kondo-insulator state below T^* . This provides the theoretical basis to understand why pressure induces a Kondo insulator to antiferromagnetic metal transition [30, 31, 43]. It also makes it at least plausible that a precursor Fermi surface appears in a Kondo insulator, similar to an inter-

pretation of the dHvA effect measured in SmB₆ [33].

In conclusion, we have determined the global phase diagram in the Kondo-insulator regime of a Kondo-lattice model. This phase diagram makes it natural that pressure tuning of Kondo insulators induces magnetic metal phases. Our results should also motivate the study of antiferromagnetic and insulator-metal quantum phase transitions in Kondo insulators with varying geometrical frustration, or with varying dimensionality through thin films or heterostructures. Finally, we have studied the momentum distribution of the single-electron excitations in the Kondo-insulator phase, and demonstrated the imprints of a small Fermi surface in this distribution.

Acknowledgements: We would like to acknowledge useful discussions with D. T. Adroja, L. Balicas, S. Sebastian, F. Steglich, A. M. Strydom, L. L. Sun, and H. von Löhneysen. This work was supported in part by JQI-NSF-PFC, LPS-MPO-CMTC, and LPS-CMTC (JHP), by the National Science Foundation of China Grant number 11374361, and the Fundamental Research Funds for the Central Universities and the Research Funds of Renmin University of China (R.Y.), by the U.S. Army Research Office Grant No. W911NF-14-1-0497 (S.P.), and by the U.S. Army Research Office Grant No. W911NF-14-1-0525, the NSF Grant No. DMR-1309531, and the Robert A. Welch Foundation Grant No. C-1411(Q.S.). J.H.P. acknowledges the hospitality of Rice University. J.H.P., S.P. and Q.S. acknowledge the hospitality of the Aspen Center for Physics (NSF Grant no. PHY-1066293) where this work was completed. The majority of the calculations have been performed on the Shared University Grid at Rice funded by NSF under Grant EIA-0216467, and a partnership between Rice University, Sun Microsystems, and Sigma Solutions, Inc..

-
- [1] H. v. Löhneysen, *J. Low Temp. Phys.* **161**, 1 (2010).
 [2] Q. Si and F. Steglich, *Science* **329**, 1161 (2010).
 [3] H. v. Löhneysen, A. Rosch, M. Vojta, and P. Wölfle, *Rev. Mod. Phys.* **79**, 1015 (2007).
 [4] A. Schröder, G. Aeppli, R. Coldea, M. Adams, O. Stockert, H. v. Löhneysen, E. Bucher, R. Ramazashvili, and P. Coleman, *Nature* **407**, 351 (2000).
 [5] S. Paschen, T. Lühmann, S. Wirth, P. Gegenwart, O. Trovarelli, C. Geibel, F. Steglich, P. Coleman, and Q. Si, *Nature* **432**, 881 (2004).
 [6] H. Shishido, R. Settai, H. Harima, and Y. Ōnuki, *Journal of the Physical Society of Japan* **74**, 1103 (2005).
 [7] S. Friedemann, N. Oeschler, S. Wirth, C. Krellner, C. Geibel, F. Steglich, S. Paschen, S. Kirchner, and Q. Si, *Proceedings of the National Academy of Sciences* **107**, 14547 (2010).
 [8] Q. Si, S. Rabello, K. Ingersent, and J. L. Smith, *Nature* **413**, 804 (2001).
 [9] P. Coleman, C. Pépin, Q. Si, and R. Ramazashvili, *Journal of Physics: Condensed Matter* **13**, R723 (2001).
 [10] Q. Si, J. H. Pixley, E. Nica, S. J. Yamamoto, P. Goswami, R. Yu, and S. Kirchner, *Journal of the Physical Society of Japan* **83**, 061005 (2014).
 [11] M. S. Kim and M. C. Aronson, *Phys. Rev. Lett.* **110**, 017201 (2013).
 [12] D. D. Khalyavin, D. T. Adroja, P. Manuel, A. Daoud-Aladine, M. Kosaka, K. Kondo, K. A. McEwen, J. H. Pixley, and Q. Si, *Phys. Rev. B* **87**, 220406 (2013).
 [13] E. D. Mun, S. L. Bud'ko, C. Martin, H. Kim, M. A. Tanatar, J.-H. Park, T. Murphy, G. M. Schmiedeshoff, N. Dille, R. Prozorov, and P. C. Canfield, *Phys. Rev. B* **87**, 075120 (2013).
 [14] V. Fritsch, N. Bagrets, G. Goll, W. Kittler, M. J. Wolf, K. Grube, C.-L. Huang, and H. v. Löhneysen, *Phys. Rev. B* **89**, 054416 (2014).
 [15] Y. Tokiwa, C. Stingl, M.-S. Kim, T. Takabatake, and P. Gegenwart, *Science Advances* **1**, e1500001 (2015).
 [16] J. Custers, K. A. Lorenzer, M. Müller, A. Prokofiev, A. Sidorenko, H. Winkler, A. M. Strydom, Y. Shimura, T. Sakakibara, R. Yu, and et. al., *Nature materials* **11**, 189 (2012).
 [17] S. Friedemann, T. Westerkamp, M. Brando, N. Oeschler, S. Wirth, P. Gegenwart, C. Krellner, C. Geibel, and F. Steglich, *Nature Physics* **5**, 465 (2009).
 [18] J. Custers, P. Gegenwart, C. Geibel, F. Steglich, P. Coleman, and S. Paschen, *Phys. Rev. Lett.* **104**, 186402 (2010).
 [19] L. Jiao, Y. Chen, Y. Kohama, D. Graf, E. Bauer, J. Singleton, J.-X. Zhu, Z. Weng, G. Pang, T. Shang, *et al.*, *Proceedings of the National Academy of Sciences* **112**, 673 (2015).
 [20] Q. Si, *Physica B: Condensed Matter* **378**, 23 (2006).
 [21] Q. Si, *Physica Status Solidi (b)* **247**, 476 (2010).
 [22] P. Coleman and A. H. Nevidomskyy, *Journal of Low Temperature Physics* **161**, 182 (2010).
 [23] J. H. Pixley, R. Yu, and Q. Si, *Phys. Rev. Lett.* **113**, 176402 (2014).
 [24] Q. Si and S. Paschen, *physica status solidi (b)* **250**, 425 (2013).
 [25] A. C. Hewson, *The Kondo problem to heavy fermions*, 2 (Cambridge university press, 1997).
 [26] G. Aeppli and Z. Fisk, *Comments Cond. Mat. Phys.* **16**.
 [27] P. S. Riseborough, *Advances in Physics* **49**, 257 (2000).
 [28] S. J. Yamamoto and Q. Si, *Journal of Low Temperature Physics* **161**, 233 (2010).
 [29] M. Dzero, K. Sun, V. Galitski, and P. Coleman, *Phys. Rev. Lett.* **104**, 106408 (2010).
 [30] A. Barla, J. Derr, J. P. Sanchez, B. Salce, G. Laperot, B. P. Doyle, R. Ruffer, R. Lengsdorf, M. M. Abd-Elmeguid, and J. Flouquet, *Phys. Rev. Lett.* **94**, 166401 (2005).
 [31] S. Gabáni, E. Bauer, S. Berger, K. Flachbart, Y. Paderno, C. Paul, V. Pavlík, and N. Shitsevalova, *Phys. Rev. B* **67**, 172406 (2003).
 [32] G. Li, Z. Xiang, F. Yu, T. Asaba, B. Lawson, P. Cai, C. Tinsman, A. Berkley, S. Wolgast, Y. S. Eo, *et al.*, *Science* **346**, 1208 (2014).
 [33] B. Tan, Y.-T. Hsu, B. Zeng, M. C. Hatnean, N. Harrison, Z. Zhu, M. Hartstein, M. Kiourlappou, A. Srivastava, M. Johannes, *et al.*, *Science* **349**, 287 (2015).
 [34] A. Auerbach, *Interacting electrons and quantum magnetism* (Springer, 1994).
 [35] B. S. Shastry and B. Sutherland, *Physica B+ C* **108**, 1069 (1981).
 [36] S. Miyahara and K. Ueda, *Journal of Physics: Condensed*

- Matter **15**, R327 (2003).
- [37] B. S. Shastry and B. Kumar, Progress of Theoretical Physics Supplement **145**, 1 (2002).
- [38] T. Kariyado and Y. Hatsugai, Phys. Rev. B **88**, 245126 (2013).
- [39] B. H. Bernhard, B. Coqblin, and C. Lacroix, Phys. Rev. B **83**, 214427 (2011).
- [40] B. H. Bernhard and C. Lacroix, Phys. Rev. B **92**, 094401 (2015).
- [41] See Supplementary Material at: .
- [42] E. M. Nica, K. Ingersent, J.-X. Zhu, and Q. Si, Phys. Rev. B **88**, 014414 (2013).
- [43] L. L. Sun et al., unpublished.

SUPPLEMENTARY MATERIAL

Here we discuss the various equations we have used in studying the nature of the Kondo insulating phase. We show the mean field parameters as a function of the Kondo coupling J_K across each phase transition in Fig. S1 (as in the phase diagram Fig. 1 of the main text) and also discuss the direct and indirect single-particle excitation gaps in the Kondo insulating phase.

EQUATIONS FOR THE SINGLE PARTICLE EXCITATIONS IN THE KONDO INSULATING PHASE

Here we give the equations for the occupation number and spectral function within our approach. In the absence of the RKKY interaction focusing on a square lattice, and after the Hubbard-Stranotovich decoupling, the Hamiltonian becomes

$$H_{MF} = \sum_{i,\alpha} i\lambda_i \left(f_{i\alpha}^\dagger f_{i\alpha} - \frac{1}{2} \right) + \sum_{\langle i,j \rangle, \sigma} t_{ij} \left(c_{i\sigma}^\dagger c_{j\sigma} + \text{h.c.} \right) + \frac{2}{J_K} \sum_i |b_i|^2 + \sum_{i,\sigma} \left(b_i^* c_{i\sigma}^\dagger f_{i\sigma} + \text{h.c.} \right).$$

Focusing on translationally invariant solutions, we can set $i\lambda_i = -\lambda$ and $b_i = b$. We can then diagonalize the Hamiltonian via Fourier transform and obtain

$$H_{MF} = H_C + \sum_{\mathbf{k}, \sigma} \left[E_{\mathbf{k}+} \gamma_{\mathbf{k}\sigma+}^\dagger \gamma_{\mathbf{k}\sigma+} + E_{\mathbf{k}-} \gamma_{\mathbf{k}\sigma-}^\dagger \gamma_{\mathbf{k}\sigma-} \right] \quad (\text{S1})$$

where the light and heavy bands (+/-) are

$$E_{\mathbf{k}\pm} = \frac{1}{2}(\epsilon_{\mathbf{k}} - \lambda) \pm \sqrt{\left(\frac{\epsilon_{\mathbf{k}} + \lambda}{2} \right)^2 + b^2}, \quad (\text{S2})$$

and

$$H_C = N \left(\frac{2}{J_K} b^2 + \lambda \right). \quad (\text{S3})$$

The quasiparticle operators, $\gamma_{\mathbf{k}\sigma\pm}$, are related to the original degrees of freedom via

$$c_{\mathbf{k}\sigma} = u_{\mathbf{k}} \gamma_{\mathbf{k}\sigma+} + v_{\mathbf{k}} \gamma_{\mathbf{k}\sigma-}, \quad (\text{S4})$$

$$f_{\mathbf{k}\sigma} = v_{\mathbf{k}} \gamma_{\mathbf{k}\sigma+} - u_{\mathbf{k}} \gamma_{\mathbf{k}\sigma-}, \quad (\text{S5})$$

where $u_{\mathbf{k}}^2 + v_{\mathbf{k}}^2 = 1$ and the form factors are

$$u_{\mathbf{k}}^2 = \frac{1}{2} + \frac{1}{2} \frac{\epsilon_{\mathbf{k}} + \lambda}{\sqrt{(\epsilon_{\mathbf{k}} + \lambda)^2 + 4b^2}}, \quad (\text{S6})$$

$$v_{\mathbf{k}}^2 = \frac{1}{2} - \frac{1}{2} \frac{\epsilon_{\mathbf{k}} + \lambda}{\sqrt{(\epsilon_{\mathbf{k}} + \lambda)^2 + 4b^2}}. \quad (\text{S7})$$

With these results in hand we can now determine the Green function of the conduction electrons,

$$G_c(\mathbf{k}, i\omega_n) = \frac{u_{\mathbf{k}}^2}{i\omega_n - E_{\mathbf{k}+}} + \frac{v_{\mathbf{k}}^2}{i\omega_n - E_{\mathbf{k}-}} \quad (\text{S8})$$

with a spectral function

$$A_c(\mathbf{k}, \omega) = u_{\mathbf{k}}^2 \delta(\omega - E_{\mathbf{k}+}) + v_{\mathbf{k}}^2 \delta(\omega - E_{\mathbf{k}-}). \quad (\text{S9})$$

Consequently, the occupation number of the c electrons at zero temperature is

$$n_{\mathbf{k}} = u_{\mathbf{k}}^2 \Theta(-E_{\mathbf{k}+}) + v_{\mathbf{k}}^2 \Theta(-E_{\mathbf{k}-}), \quad (\text{S10})$$

where $\Theta(x)$ is the Heaviside step function. From the Green function we can also determine the quasiparticle residue in the heavy Fermi liquid phase for the filling $n_c = 1.25$ as in the main text. In the heavy Fermi liquid phase the total filling will be $n_c + n_f = 2.25$, hence $E_{\mathbf{k}_F^*+} = 0$ and there is only a pole at $E_{\mathbf{k}_F^*-}$ away from zero energy. Therefore, the residue for the c and f electrons at the Fermi energy is $z_c = v_{\mathbf{k}_F^*}^2$, and $z_f = u_{\mathbf{k}_F^*}^2$ respectively.

MEAN FIELD PARAMETERS

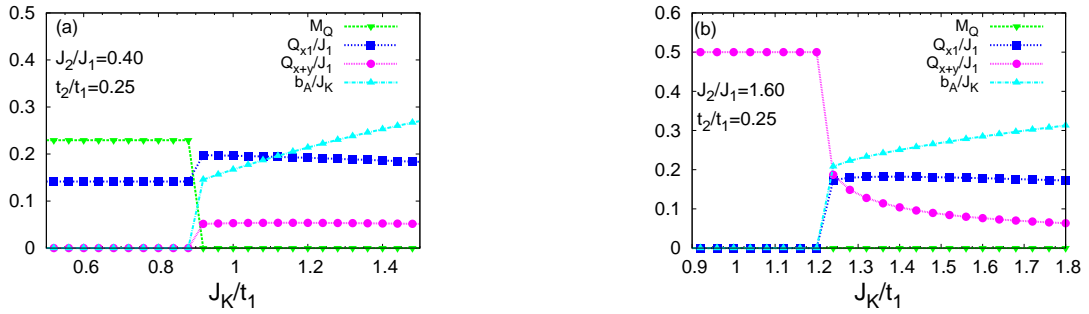


FIG. S1. Mean field parameters across each of the Kondo insulating to Kondo destroyed transitions for $t_2 = 0.25t_1$. (Only the distinct parameters are shown.) (a) For the AF_S to KI phase transition as a function of the Kondo coupling J_K for $J_2/J_1 = 0.4$. We find a direct first order transition between the AF_S and KI phase signaled by a vanishing of the magnetic order parameter $M_{\mathbf{Q}}$ (where \mathbf{Q} corresponds to the AF wave vector); (b) Mean field parameters for the SSL-VBS to KI phase transition as a function of the Kondo coupling J_K for $J_2/J_1 = 1.6$. We find a direct first order transition between the VBS and KI phase.

DIRECT AND INDIRECT GAPS

We define the direct gap ($\Delta E \equiv \min \Delta E_{\mathbf{k}}$), which captures the lowest lying excitations that don't change momentum. Likewise, we define the indirect gap ($\delta E \equiv \min E_{\mathbf{k}+} - \max E_{\mathbf{k}-}$), which corresponds to the lowest-energy excitation when the momentum is allowed to change. In Fig. S2 (a), we show the direct gap as a function of the Kondo coupling J_K , which has the expected exponential dependence. Compared to the indirect gap, which is of the order of the Kondo temperature, the direct gap is larger and has a square-root dependence on the latter, as is shown in Fig. S2 (b).

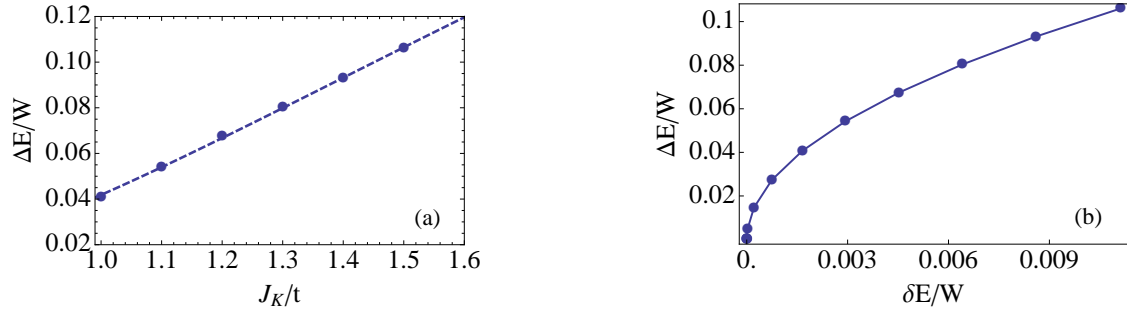


FIG. S2. Direct and indirect gaps in the Kondo insulating phase. (a) Direct gap ΔE as a function of the Kondo coupling J_K . Here, the dashed line is a fit to the expected exponential form $[a \exp(-b/J_K)]$. (b) The direct gap as a function of the indirect gap δE , satisfying $\Delta E \sim \sqrt{\delta E}$.